Biochem. J. (1978) **171**, 375–383
Printed in Great Britain

Processing and Migration of Ribosomal Ribonucleic Acids in the Nucleolus and Nucleoplasm of Rat Liver Nuclei

By KALIN P. DUDOV, MARIANA D. DABEVA and ASEN A. HADJIOLOV
Department of Molecular Genetics, Institute of Molecular Biology, Bulgarian Academy of Sciences, 1113 Sofia, Bulgaria

and

BORISLAV N. TODOROV
Department of Radiobiology, Higher Institute of Veterinary Medicine, Stara Zagora, Bulgaria

(*Received* 12 *August* 1977)

Kinetic studies on the labelling *in vivo* with [^{14}C]orotate of rat liver nucleolar and nucleoplasmic pre-rRNA (precursor of rRNA) and rRNA, isolated from detergent-purified nuclei, were carried out. The mathematical methods used for the computer analysis of specific-radioactivity curves are described. Evaluation of the experimental data permitted the selection of the most probable models for the processing of pre-rRNA and the nucleo-cytoplasmic transfer of rRNA. It was shown that considerable flexibility exists in the sequence of endonuclease attacks at critical sites of 45 and 41 S pre-rRNA chains, resulting in the simultaneous occurrence of several processing pathways. However, the phosphodiester bonds involved in the formation of mature 28 and 18 S rRNA appear to be protected until the generation of their immediate pre-rRNA. The turnover rates and half-lives of all pre-rRNA and rRNA pools were determined. The turnover rate of 45 S pre-rRNA corresponds to the formation of 1100 ribosomes/min per nucleus. The model for the nucleolus–nucleoplasm–cytoplasm migration of rRNA includes a 'nucleoplasm' compartment in which the small ribosomal subparticle is in rapid equilibrium with the respective cytoplasmic pool. At equimolar amounts of nuclear 28 and 18 S rRNA this model explains the faster appearance of labelled small ribosomal subparticles in the cytoplasm simultaneous with a lower labelling of nuclear 18 S rRNA as compared with 28 S rRNA.

The identification and molecular characteristics of pre-rRNA species in eukaryotes led to the proposal of intranuclear processing pathways for the formation of mature ribosomes (see Perry, 1976; Hadjiolov & Nikolaev, 1976). In general, the process seems to involve four major endonuclease attacks at critical sites along pre-rRNA chains (Perry, 1976; Hadjiolov, 1977). It is thought that endonuclease attacks follow a rigid sequential pattern generating a single pre-rRNA-processing pathway for a given cell type. However, evidence for variations in the temporal order of endonuclease attacks and the simultaneous existence of more than one processing pathway was obtained with a variety of animal cells (Weinberg & Penman, 1970; Purtell & Anthony, 1975; Winicov, 1976; Toniolo & Basilico, 1976; Dabeva *et al.*, 1976*b*). These findings raise the question about the actual precursor–product relationships in pre-rRNA maturation. An adequate answer to this question requires the quantitative analysis of detailed labelling-kinetics data. In the present work, we studied the turnover of nuclear pre-rRNA and rRNA species in rat liver as a model of non-growing animal cells, operating under steady-state conditions. Advantage was taken of the good resolving power of urea/agar-gel electrophoresis (Dudov *et al.*, 1976), which permits one to obtain reasonably accurate specific-radioactivity curves. An algebraic approach to the computer analysis of tracer-kinetics data, involving a large number of pools, was developed and adequacy criteria were defined, which allows selection of the most probable state of the existing connections among pools. The results obtained made possible the proposal of models for pre-rRNA processing and nucleolus – nucleoplasm – cytoplasm migration of rRNA.

Abbreviations used: pre-rRNA, precursor of rRNA; nuRNA, nucleolar RNA; npRNA, nucleoplasmic RNA.

Theory

Basic equations

The basic principles for the analysis of tracer-kinetics experiments are given by Sheppard & Householder (1951), Reiner (1953), Zilversmith

(1960) and Sheppard (1962). When applied to the study of a system of n interconnected and homogeneous RNA pools, labelled in one nucleotide, they give the equations:

$$A_i\frac{dS_i(t)}{dt}=\sum_{j=1}^{n}v_{ji}\left(\frac{\beta_i}{\beta_j}S_j-S_i\right),\qquad i=1,2,\ldots,n;\quad(1)$$

where S_i (c.p.m./pg) is the specific radioactivity of RNA in pool i, A_i (pg) is the size of pool i, v_{ji} (pg/min) is the rate of transfer from pool j into pool i; β_i is the percentage of the labelled nucleotide in the RNA molecules from pool i. Under our conditions of analysis of a steady-state system, the following equations are valid:

$$A_i=\text{const.},\quad \sum_k v_{ki}=\sum_m v_{im},\ i=1,2,\ldots,n;\quad(2)$$

and

$$v_{ji}=\text{const.},\quad i,j=1,2,\ldots,n\ (i\neq j).\quad(3)$$

When A_i, β_i ($i=1,2,\ldots,n$) are known and we have a good approximating function $S_i(t)$ ($i=1,2,\ldots,n$) for the experimentally determined specific-radioactivity points, the calculation of the unknown rates (v_{ji}) is reduced to the solution of the algebraic equations:

$$S_i(t_l)-S_i(t_1)=\sum_{j=1}^{n}\frac{v_{ji}}{A_i}\int_{t_1}^{t_l}\left(\frac{\beta_i}{\beta_j}S_j-S_i\right)dt,\qquad i=1,2,\ldots,n;\quad(4)$$

where the RNA pools are analysed in the time interval (t_1, t_l).

It is known that specific-radioactivity curves are most informative at early time intervals when the system as a whole is far from the isotopic steady-state (Sheppard, 1962). During these time intervals all curves increase monotonously and cannot have more than one inflection point. Therefore we use a third-degree polynome for $S_i(t)$, which in our case gives a good approximation to experimental data. The introduction of multi-exponential functions for $S_i(t)$ does not influence the rate values when obtained by the simulation method described below.

The steady-state conditions (eqn. 2) and the knowledge of possible relationships between pre-rRNA and rRNA pools were sufficient to supply the necessary additional relations between the rates to solve eqn. (4) as a determined algebraic system.

Evaluation of transfer rates and their errors

Repeated determinations of the size of all pools (A_i) and their specific radioactivities (s_{ir}) for each labelling term (t_r) permit the calculation of S.D. for A_i and s_{ir}: $\sigma(A_i)$ and $\sigma(s_{ir})$, ($i=1,2,\ldots,n$; $r=1,2\ldots,l$). This makes possible the application of a data-simulation procedure for the evaluation of transfer rates and their errors (Myhill, 1967; Atkins, 1972). For a given pool i and each sampling point t_r we generate a normally distributed random number with mean s_{ir} and S.D. $\sigma(s_{ir})$. The specific-radioactivity points obtained are approximated with a cubic polynome $S_i(t)$. This Monte Carlo procedure allows us to generate a set of n specific-radioactivity curves permitted by the experimental error in the determination of all s_{ir}. A set of such pseudo-random curves gives a set of values for $k_{ji}=v_{ji}/A_i$. By repeating this process we can calculate the average $\bar{k}_{ji}$ and their S.D. $\sigma(\bar{k}_{ji})$. If we consider $\bar{k}_{ji}$ and A_j as independent variables, the respective rates are designated $\bar{v}_{ji}$ and calculated from $\bar{v}_{ji}=\bar{k}_{ji}A_i$. The experimental error in the determination of the pool sizes is included in the S.D. of the rates by the equation:

$$\sigma(\bar{v}_{ji})=\{[\sigma(A_i)\bar{k}_{ji}]^2+[\sigma(\bar{k}_{ji})A_i]^2\}^{0.5}$$

The values obtained allow us to calculate the pool characteristics corresponding to the model tested (Zilversmith, 1960):

(*a*) Turnover rate:

$$V_i^T=\sum_k\bar{v}_{ik},\ \sigma(V_i^T)=\left[\sum_k\sigma(\bar{v}_{ik})\right]^{0.5}$$

(*b*) Turnover time:

$$T_i=A_i/V_i^T,\ \sigma(T_i)=A_i\sigma(V_i^T)(V_i^T)^{-2}$$

(*c*) Half-life time:

$$T_i^{1/2}=\ln 2\times T_i,\ \sigma(T_i^{1/2})=\ln 2\times\sigma(T_i).$$

Adequacy criteria

A model of pre-rRNA maturation is defined as a given state of the connections between separate pre-rRNA and rRNA pools and a set of constraints on the unknown transfer rates. We used the following adequacy criteria to select the most probable model.

(Cr_1). The transfer-rate values for each model tested should satisfy the requirement for a steady-state system (eqn. 2). The zero hypothesis

$$H_0\left(\sum_k\bar{v}_{ki}=\sum_m\bar{v}_{im}\right)$$

should be examined for each pool i by Student's t test. If H_0 is rejected, the tested model is considered inconsistent. The statistical significance of the obtained transfer-rate values ($\bar{v}_{ji}$) is tested by the same method.

(Cr_2). After determination of $\bar{v}_{ji}$ we can solve eqn. (1) and obtain the theoretical curves $S_i^{\text{theor.}}$ at initial conditions $S_i^{\text{theor.}}(t_1)=S_i(t_1)$. The requirement for a best fit of the model to all experimental points is given by:

$$W^2=\sum_{i=1}^{n}\sum_{r=1}^{l}\left(\frac{S_i^{\text{theor.}}(t_r)-s_{ir}}{S_i(t_r)}\right)^2=\text{minimum}$$

If we test two models A and B, we can use the statistical F test to check H_0 ($W_A^2=W_B^2$). If this hypothesis is rejected, we prefer the model giving a lower value for W^2.

(Cr_3). If the whole time interval (t_1, t_l) is divided in m ($m<l$, $t_{m+1} \equiv t_l$) subintervals (t_k, t_{k+1}), ($k=1, 2, \ldots, m$), we can write m algebraic systems (eqn. 4). Their solution (simultaneously with the introduced constraints on the rates) gives m sets of values v_{jl}^k ($k=1, 2, \ldots, m$) and the average $\bar{v}_{jl}^k$ ($k=1, 2, \ldots, m$) can be calculated from all simulation cycles. Thus (Cr_3) is derived from eqn. (3) and is defined as a requirement for a minimal variation of the rates among time subintervals:

$$\sum_{j,l} \sigma^2(v_{jl}^{\text{int.}}) = \min.$$

where

$$v_{jl}^{\text{int.}} = \frac{1}{m} \sum_{k=1}^{m} \bar{v}_{jl}^k.$$

When two models satisfy (Cr_1) and (Cr_2) to an equal extent then according to (Cr_3) we prefer the model involving a smaller number of constants. The simultaneous presence of higher ($v^{\text{int.}}$) values for all in-flow rates of a given pool indicates the introduction of superfluous constants in the mathematical description of this pool.

Evaluation of cross-contamination between neighbour compartments

Let us consider two subsequent compartments i and $i+1$ from the terminal catenary segment of a pool system, where we have determined experimentally A_i, A_{i+1}, $s_i(t)$ and $s_{i+1}(t)$. When the analysis of preceding pools allows us to determine all in-flow rates (v_{ki}) to compartment i, we can calculate the percentage ($p_i \times 100$) contamination in pool i by molecules from pool $i+1$. We designate by A_i^d, A_{i+1}^d, s_i^d and s_{i+1}^d the actual amounts and specific radioactivities in these pools, so:

$$A_i^d = A_i(1-p_i),\ A_{i+1}^d = A_{i+1} + p_i A_i,\ s_{i+1}^d = s_{i+1}$$

For each $t \in (t_1, t_l)$, the total radioactivity in the pool i is

$$R(p_i,t) = p_i A_i s_{i+1}(t) + A_i(1-p_i)\, s_i^d(t)$$

where $s_i^d(t)$ is derived from:

$$A_i^d \frac{ds_i^d}{dt} = \sum_k v_{ki} \left(\frac{\beta_l}{\beta_k} s_k - s_i^d \right)$$

at initial condition:

$$s_i^d(t_1) = \frac{[s_i(t_1) - s_{i+1}(t_1)p_i]}{(1-p_i)}$$

In this way the solution of the problem is reduced to the finding of a p_i' which will satisfy the requirement:

$$R(p_i') = \left| \int_{t_1}^{t_l} [R(p_i',t) - s_l(t)A_i]dt \right| = \min.$$

The optimal value for p_i can be numerically calculated with the required accuracy by introducing subsequent values for p from 0 to 1 with an appropriate step.

Experimental

The labelling-kinetics experiments were carried out with Wistar male albino rats weighing 150±5g. Labelling *in vivo* was with 25μCi of [^{14}C]orotate (specific radioactivity 19mCi/mmol) per rat for 20–140min, with eight animals per experimental point. Isolation of detergent-purified nuclei and extraction of nucleolar (nuRNA and 50°C nuRNA) and nucleoplasmic (npRNA and 4°C npRNA) fractions was carried out as described in the preceding paper (Dabeva *et al.*, 1978). The amount of each pre-rRNA and rRNA component was determined by its A_{260} after fractionation of these RNA fractions by urea/agar-gel electrophoresis (Dudov *et al.*, 1976). The dried agar-gel films were cut in 1mm slices and RNA was solubilized with 0.5ml of 2.5% (v/v) NH_3 for 24h at 25°C. Excess of NH_3 was evaporated and to each sample were added 4.5ml of a mixture containing 1vol. of Triton X-100 (scintillation grade) and 2vol. of a toluene/2,5-diphenyloxazole/dimethyl-POPOP [1,4-bis-(4-methyl-5-phenyloxazol-2-yl)/benzene] phosphor (Dabeva *et al.*, 1976*a*). The samples were counted for radioactivity in a Packard Tri-Carb 3320 liquid-scintillation spectrometer. The specific radioactivity of each pre-rRNA and rRNA peak was calculated from the radioactivity determined and the A_{260} area corresponding to the respective gel slices (see Dabeva *et al.*, 1978), and expressed as c.p.m./A_{260} unit. Average values of three to five independent electrophoretic runs for each RNA sample were calculated.

Results and Discussion

Maturation pathways of pre-rRNA in the nucleolus

In rat liver the following pools of nucleolar rRNA were identified: 45, 41, 39, 36, 32 and 21 S pre-rRNA plus 28 and 18 S rRNA (Dabeva *et al.*, 1976*b*). The pool sizes of these pre-rRNA and rRNA were determined (Dabeva *et al.*, 1978) and their nucleotide composition is known (Dabeva & Tsanev, 1968). In Fig. 1 the labelling-kinetic curves (20–140min) for liver pre-rRNA and rRNA species obtained from parallel analyses of nuRNA and 50°C nuRNA (see Dabeva *et al.*, 1978) are given. On the basis of existing knowledge (Busch & Smetana, 1970: Hadjiolov & Nikolaev, 1976) and our experimental data, the system analysed here is characterized as follows.

(*a*) Maturation starts with 45 S pre-rRNA considered as the only primary pre-rRNA molecule. Short-term (10min) labelling experiments *in vivo*

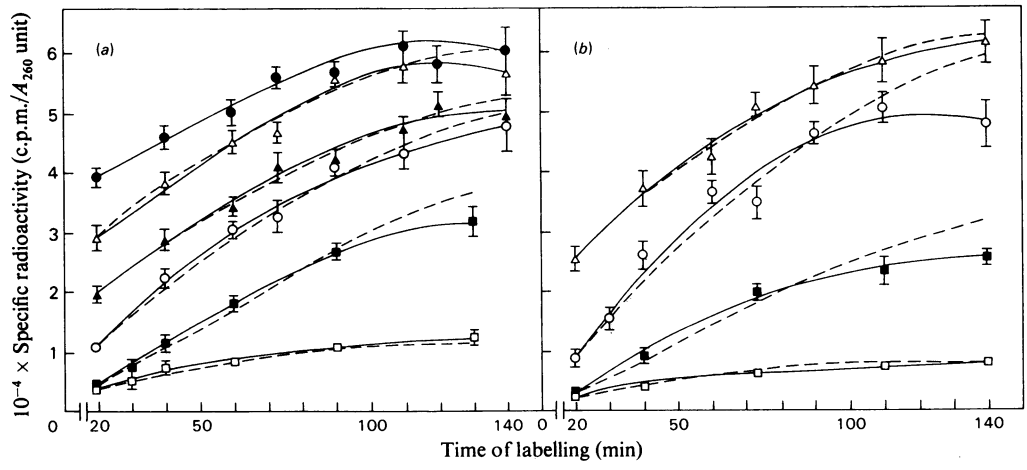

Fig. 1. *Kinetics of labelling of liver nucleolar pre-rRNA and rRNA in vivo*

The experimental points represent mean values obtained from the analysis of nuRNA and 50°C nuRNA (three to five experiments) given with their S.D. (vertical bars). ——, Experimental curves obtained by a third-degree polynomial approximation; – – – –, theoretical curves corresponding to the most probable model shown in Fig. 2. The amount of pre-rRNA pool is taken from Dabeva *et al.* (1978). The theoretical curves for 28 and 18 S rRNA are based on amounts corrected for cross-contamination by the respective nucleoplasmic pools, as given in Table 3. (*a*) 45 S (●), 41 S (△), 36 S (▲) and 32 S (○) pre-rRNA; 28 S (■) and 18 S (□) rRNA in nuRNA. (*b*) 39 S (△) and 21 S (○) pre-rRNA; 28 S (■) and 18 S (□) rRNA in 50°C nuRNA.

with high doses of [^{14}C]orotate reveal that more than 90% of the radioactivity in nuRNA is confined to 45 S pre-rRNA (results not shown).

(*b*) The system is open only at the entrance point (45 S pre-rRNA) and the exit points (nucleolar 28 S and 18 S rRNA), i.e. degradation of conserved sequences in intermediate pre-rRNA is not considered (see Wolf & Schlessinger, 1977). For liver, evidence for the validity of this assumption is given by the established equal decay rates for the two ribosomal subparticles (Hadjiolov, 1966; Tsurugi *et al.*, 1974; Eliceiri, 1976).

(*c*) The kinetic curves are analysed for the first 100 min, since at longer times of labelling they approach isotopic saturation and their informative value is limited (Sheppard, 1962).

(*d*) For the above periods of labelling most of the label in RNA is in UMP, the values for labelled CMP being negligible (Hadjiolov *et al.*, 1967).

(*e*) Generation of 36 S pre-rRNA is simultaneous with the formation of 18 S rRNA, and that of 32 S pre-rRNA with 21 S pre-rRNA (Dabeva *et al.*, 1976*b*).

(*f*) The polarity in the labelling of primary pre-rRNA (Hadjiolov & Milchev, 1974) does not interfere substantially at labelling periods longer than 20 min. Under our conditions (see Fig. 1) the label in 45 S pre-rRNA beyond this term increases slowly, which indicates the absence of rapid changes in the specific radioactivity of UTP. On the other hand, the presence of labelled 18 S rRNA in liver cytoplasm at 10 min (Chaudhuri & Lieberman, 1968) indicates a relatively high rate of RNA polymerase A recycling on transcribed rRNA genes. Therefore at labelling times longer than 20 min pre-rRNA and rRNA are considered homogeneously labelled along their chains.

The available information on pre-rRNA processing shows that it is the result of a limited number of endonuclease attacks at critical sites along the polynucleotide chain (see Hadjiolov & Nikolaev, 1976). Recent evidence reveals some flexibility in the sequence of endonuclease attacks and the simultaneous existence of more than one pre-rRNA-maturation pathways (see Winicov, 1976; Dabeva *et al.*, 1976*b*). These findings make it necessary to analyse all possible precursor–product relationships among pre-RNA species. Thus a general model of pre-rRNA processing implies the possibility for each pre-rRNA molecule to be split simultaneously at all of its critical sites. By the omission of some phosphodiester-bond splits at a given maturation step a series of different models are generated. The mathematical methods described in the Theory section were used to build a computer program for the analysis of all possible models of pre-rRNA processing in rat liver postulated in accordance with characteristics (*a*) to (*f*). This program allows us to determine all transfer rates (v_{ji}) in a given model and to test it in relation to criteria (Cr_1) to (Cr_3). Know-

ledge of molecular weights of liver pre-rRNA species (Dabeva *et al.*, 1976*b*) permits expression of v_{ji} in number of molecules/min. The analysis of one such model in which 41 S pre-rRNA is the only immediate product of 45 S pre-rRNA was of particular interest, since it is generally assumed that this is the first maturation step in animal cells (see Hadjiolov & Nikolaev, 1976). However, when tested this model did not satisfy simultaneously (Cr_1) to (Cr_3). For example, the estimated rate of 41 S pre-rRNA formation (350mol/min per nucleus) is about one-quarter of the respective outflow rate (1350mol/min per nucleus), a value well beyond the experimental error and not satisfying (Cr_1). Consequently, this model has to be rejected as incompatible with our experimental data.

The most probable model of pre-rRNA maturation in rat liver derived from our studies is presented in Fig. 2. This model satisfies simultaneously (Cr_1) to (Cr_3), and the good fit between theoretical and experimental kinetic curves is seen in Fig. 1. A major feature of the proposed model is the possibility for independent endonuclease attack at all four critical sites in the 45 S pre-rRNA chain. The corresponding values for transfer rates (v_{ji}) are given in Table 1 and permit the calculation of turnover rates and half-lives for the separate nucleolar pre-rRNA pools (Table 2). Quantitative data in the literature on the turnover of pre-rRNA species are scarce and indirect in most cases. Nevertheless, our results are in good agreement with published values on the half-life of liver 45 S pre-rRNA (Muramatsu *et al.*, 1966) and HeLa-cell 45 and 32 S pre-rRNA (Wolf & Schlessinger, 1977). The rate of synthesis of liver ribosomes (1100mol/min per nucleus) derived from our results is close to reported values for growing fibroblasts (Emerson, 1971), but is lower than those for L and HeLa cells (Brandhorst & McConkey, 1974; Wolf & Schlessinger, 1977) and severalfold higher than determined for rabbit erythroid cells (Hunt, 1976).

Our results demonstrate that considerable flexibility exists in the sequence of endonuclease attacks at critical sites in pre-rRNA molecules and that several pre-rRNA-processing pathways operate

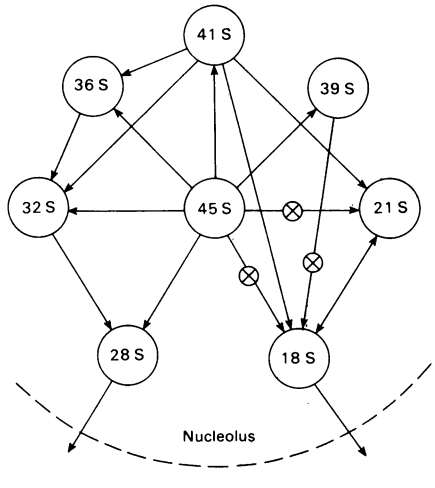

Fig. 2. *Most probable model of pre-rRNA maturation in rat liver nucleoli*

The model is derived from computer analysis of specific-radioactivity kinetics curves and size of nucleolar pre-rRNA and rRNA pools, as well as knowledge of molecular weights, topology and nucleotide composition of the respective molecules. The arrows indicate possible conversions involved in pre-rRNA maturation with statistically significant transfer rates. ⊗, Unidentified intermediate pre-rRNA pools containing a 24 S RNA segment, characterized by a very fast turnover. For details see the text and Fig. 3.

Table 1. *Transfer rates between pre-rRNA and rRNA pools in rat liver nucleolus*

The separate transfer rates v_{ji} are obtained by computer analysis of the most probable model given in Fig. 2. The percentage error is calculated from $\sigma(v_{ji})\times 100/v_{ji}$, where $\sigma(v_{ji})$ is the S.D. of v_{ji}.

Transfer between pools		Transfer rates	Percentage
from	into	(mol/min per nucleus)	error
45 S	41 S	360	44
	39 S, 28 S	×120	34
	36 S, 18 S	×270	72
	32 S, 21 S	×360	88
41 S	36 S, 18 S	×140	80
	32 S, 21 S	×220	94
39 S	18 S	120	45
36 S	32 S	410	47
32 S	28 S	1000	41
21 S	18 S	590	61

Table 2. *Turnover rates and half-lives of rat liver nucleolar pre-rRNA pools*

The values obtained correspond to the most probable model of pre-rRNA maturation shown in Fig. 2. The percentage error is calculated as in Table 1.

Pre-rRNA pool	Turnover rate (mol/min per nucleus)	Half-life (min)	Percentage error
45 S	1100	7.2	38
41 S	360	13.4	126
39 S	120	17.6	45
36 S	410	19.9	46
32 S	1000	20.3	41
21 S	590	29.4	61

simultaneously in the cell. The probability for endonuclease attack at a given critical site in 45 and 41 S pre-rRNA, computed on the basis of our model, is represented in Fig. 3. Evaluation of these results shows that endonuclease attack at sites 1, 2 and 3 in 45 S pre-rRNA occurs with a markedly higher probability than at site 4. Further, analysis of models involving the conversions 41 S pre-rRNA→28 S rRNA or 36 S pre-rRNA→28 S rRNA permitted their rejection, since the derived transfer rates are negligibly small. These results indicate that site 4 is protected from endonuclease attack until the formation of 32 S pre-rRNA. Similar more rigid requirements may operate in the formation of 18 S rRNA, since more than 50% of these molecules are generated via 21 S pre-rRNA. The factors determining the different probabilities for endonuclease attack along pre-rRNA chains and the physiological role of the resulting processing pathways remain to be elucidated.

Further, Fig. 4 shows that a linear correlation can be established between the turnover rate and the total number of endonuclease-attack sites in a given pre-rRNA pool. This indicates that pre-rRNA processing may be considered as a first-order enzymic reaction and the rate constant for the conversion of all pre-rRNA species is of the same order (about 0.03 min^{-1}).

Migration of 28 S and 18 S rRNA in the nucleolus and nucleoplasm

The labelling-kinetics curves for rat liver nucleolar and nucleoplasmic 28 and 18 S rRNA are given in

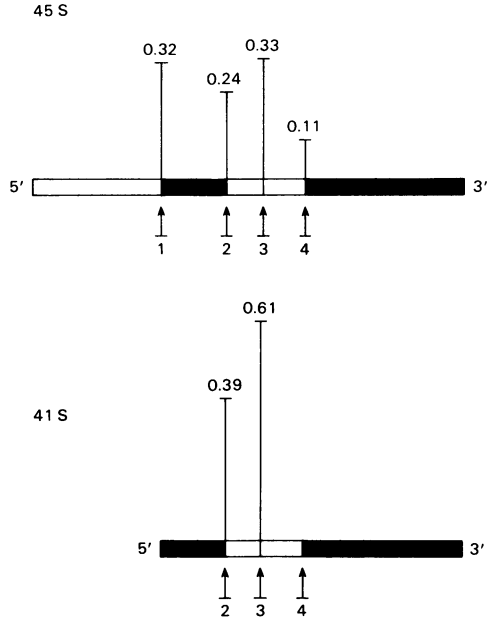

Fig. 3. *Probabilities of endonuclease splits at critical sites of 45 and 41 S pre-rRNA corresponding to the model given in Fig. 2*

Schemes of 45 and 41 S pre-rRNA showing the location of 18 and 28 S rRNA segments (in black) and of external and internal transcribed spacers (in white). The arrows indicate the sites of endonuclease attack. The probability of endonuclease attack at a given site (vertical lines) are calculated from data given in Table 1. Endonuclease attacks of 45 S pre-rRNA generate the following: site 1, 41 S pre-rRNA; site 2, 36 S pre-rRNA+unidentified precursor of 18 S rRNA; site 3, 32 S pre-rRNA+unidentified precursor of 21 S rRNA; site 4, 28 S rRNA+39 S pre-rRNA. Endonuclease attacks of 41 S pre-rRNA generate the following: site 2, 36 S pre-rRNA+18 S rRNA; site 3, 32 S+21 S pre-rRNA; site 4, 28 S rRNA+unidentified precursor of 18 S rRNA. It is noteworthy that the probability of endonuclease attack at site 4 is very low at the stage of 45 S, and about 0 at the stage of 41 S pre-rRNA.

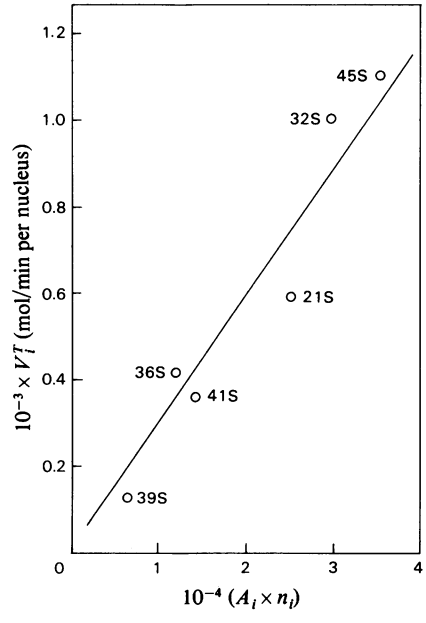

Fig. 4. *Correlation between the turnover rate V_i^T of pool i and total amount of critical sites of endonuclease attack $(A_i \times n_i)$ in the same pool*

A_i, size of pool i (no. of molecules); n_i, no. of critical sites with a high probability of endonuclease attack according to the model given in Fig. 2. The enzymic processing of pre-rRNA molecules may be considered as a first-order reaction:

$$-\frac{dA_i}{dt} = V_i^T = k(A_i \times n_i),$$

with a rate constant $k \approx 0.03$ min^{-1}.

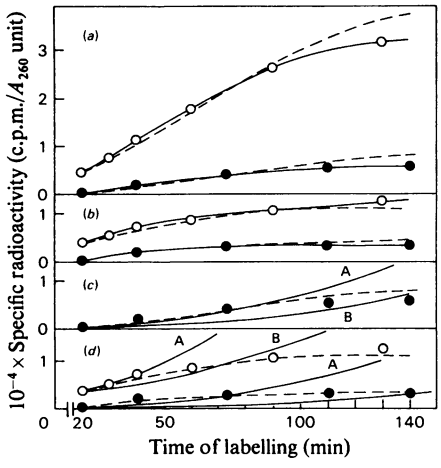

Fig. 5. *Kinetics of labelling of* 28 *and* 18 *S rRNA in the nucleolus and nucleoplasm compartments*
The experimental points for 28 and 18 S rRNA in the nucleolus (○) and the nucleoplasm (●) are given. The experimental curves (——) for 28 S (*a*) and 18 S (*b*) rRNA are obtained by approximation with third-degree polynomes. The theoretical curves (– – – –) are based on the corrected amounts of rRNA given in Table 3 and the model shown in Fig. 6. In (*c*) and (*d*), theoretical curves (– – – –) based on the model shown in Fig. 6 are compared with the theoretical curves (——) obtained by postulating 50% (A) or 80% (B) degradation of rRNA at the stage of the respective immediate precursor pool, for 28 S (*c*) and 18 S (*d*) rRNA.

Fig. 5. The pronounced differences in the specific radioactivities of nucleolar and nucleoplasmic 28 S rRNA demonstrate the existence in the nucleus of two distinct compartments. This difference is less clear-cut for 18 S rRNA (see below). The curves for 28 and 18 S rRNA reach isotopic saturation at times when the labelling of their immediate precursors is still rising (see Fig. 1). This fact reveals that dilution of the label in the pools of nucleolar and nucleoplasmic rRNA is taking place (Zilversmith, 1960; Reiner, 1974).

The possibility that the large difference between labelling curves is due to degradation at stages pre-rRNA→18 S nu-rRNA, 18 S nu-rRNA→18 S np-rRNA and 28 S nu-rRNA→28 S np-rRNA was analysed, and the results are shown in Figs. 5(*c*) and 5(*d*). It is evident that degradation alone cannot explain the character of the experimental curves. Therefore we can consider isotopic dilution as the major factor involved. This dilution may reflect: (*a*) contamination of each rRNA pool by molecules from the next compartment, i.e. nucleoplasm→nucleolus and cytoplasm→nucleoplasm; and (*b*) existence of a diffusion equilibrium *in vivo* between the rRNA pools in these compartments. The proposed quantitative model of pre-rRNA maturation allows us to estimate the amount of 28 and 18 S rRNA in the nucleolar and nucleoplasmic pools on the basis of their kinetics of labelling. In Table 3 the computed values are compared with direct estimates based on A_{260} measurements, as well as with values derived from long-term-labelling experiments. Com-

Table 3. *Estimated amounts of* 28 *and* 18 *S rRNA in the nucleolus and nucleoplasm compartments of rat liver nuclei*
The amounts of 28 and 18 S rRNA in the nucleolus and nucleoplasm compartments are determined by direct A_{260} measurements (Method I) and are corrected by using different isotopic labelling techniques. For Method II, the amount of contaminating cytoplasmic ribosomes is estimated by isotopic dilution (Dabeva *et al.*, 1977). In Method III, amounts of rRNA are calculated on the basis of long-term labelling experiments. Liver RNA is labelled *in vivo* with [^{14}C]orotate for 6 days and the specific radioactivity of 45 S pre-rRNA, 28 and 18 S rRNA in the nucleolus, nucleoplasm and cytoplasm compartments is determined. The correction is based on the assumption that at this term of labelling the specific radioactivities of nuclear 45 S pre-rRNA and rRNA should be equal. Method IV gives amounts of rRNA after correction based on the analysis of tracer-kinetics curves (see the text).

			10^{-4} × No. of molecules per nucleus			
rRNA species	Nuclear fraction	Method . . .	I	II	III	IV
28 S	nuRNA		4.5	3.7	—	4.1
	50°C nuRNA		5.1	4.2	4.8	3.5
	npRNA		8.9	5.9	—	2.5
	4°C npRNA		8.5	5.7	1.4	2.4
	Whole nuclei		13.5	9.6	6.2	6.3
18 S	nuRNA		3.8	2.6	—	0.6
	50°C nuRNA		6.2	4.3	1.4	0.6
	npRNA		9.8	6.1	—	0.8
	4°C npRNA		7.1	4.3	0.4	0.8
	Whole nuclei		13.4	8.7	1.8	1.4
28 S/18 S	Whole nuclei		1.0	1.1	3.4	4.5

parison of the values for the amount of nuclear rRNA pools obtained by different methods show that the pool of nucleolar 28 S rRNA is free of appreciable contamination. Our data show also that total nuclear 28 S rRNA may be contaminated at most by an equal amount of cytoplasmic 28 S rRNA. On the other hand, according to labelling data, both nucleolar and nucleoplasmic 18 S rRNA may be contaminated to a markedly higher extent. This fact makes uncertain the distinction between nucleolar and nucleoplasmic pools of 18 S rRNA and requires their consideration as a common nuclear pool.

It is remarkable that the nuclear 28 S/18 S rRNA molar ratio is about 1.0 when determined by A_{260}, but it is 4.5 when derived from labelling-kinetics experiments, a finding reflecting the markedly lower total label in nuclear 18 S rRNA. Such low estimates for nuclear 18 S rRNA, based on tracer studies, have been reported also for HeLa cells (Penman, 1966; Penman *et al.*, 1966; Vaughan *et al.*, 1967), whereas a 28 S/18 S rRNA molar ratio of only 1.2 was found by A_{260} measurement (Weinberg *et al.*, 1967; Weinberg & Penman, 1968). Since the amount of true nuclear 28 S rRNA is equal to that of possible contaminants, the observed large discrepancy in estimated 28 S/18 S rRNA molar ratios is beyond the experimental error and cannot be explained by postulating negligibly small amounts of true nuclear 28 S and 18 S rRNA. One possible explanation may be that detergent-purified nuclei are contaminated by an about 4-fold higher amount of small ribosomal subparticles. This explanation is highly unlikely, since it is known that the large subparticle is more tightly bound to membranes and a 1:1 molar ratio is found for the two subparticles in contaminating cytoplasmic ribosomes (Smith *et al.*, 1969; Dabeva *et al.*, 1977). Therefore neither cytoplasmic contamination nor degradation alone (see above) could explain our experimental findings. Consequently, we propose an alternative explanation which accepts the existence of a rapid exchange of ribosomal subparticles between the 'nucleoplasm' and cytoplasm compartments of the cell. Our computer program permits evaluation of the exchange rates giving a best fit to experimental kinetic curves (see Figs. 5*a* and 5*b*). The derived model for the migration of 28 and 18 S rRNA is given in Fig. 6.

In our model we consider an intranuclear 28 S/18 S rRNA molar ratio close to 1 and the minimal amount of true nuclear 28 S rRNA. We also introduce an additional compartment constituted by ribosomes that resist detergent treatment of nuclei. These ribosomes are constituents of our nucleoplasmic fraction and may be related to the ones removed from detergent-purified nuclei by DNA or polyanion treatment (Bach & Johnson, 1967; Goidl *et al.*, 1975). Yet this compartment is in rapid exchange with the pools of free cytoplasmic ribosomal subparticles and is therefore composed of ribosomes associated with the outer nuclear membrane, although we cannot rule out the possibility that it may belong to the nuclear-pore complex or be truly intranuclear. The exchange rates for the two ribosomal subparticles in this compartment can be computed and the results indicate

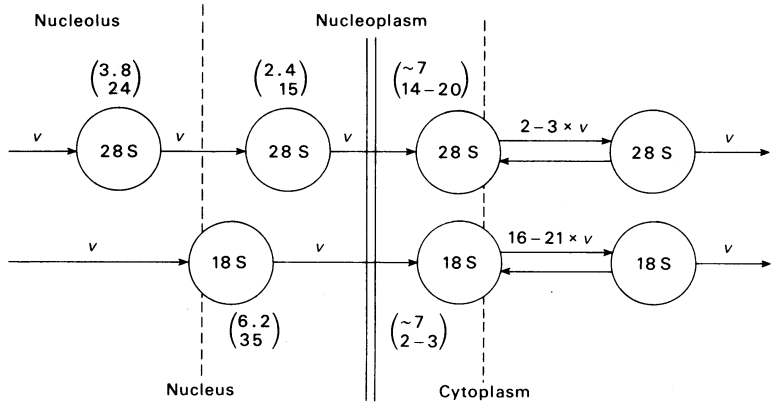

Fig. 6. *Model for the nucleolus–nucleoplasm–cytoplasm transitions of* 28 *and* 18 *S rRNA*
The model includes a 'nucleoplasmic' compartment in detergent-purified nuclei constituted by (*a*) true intranuclear rRNA and (*b*) rRNA probably associated with the nuclear membrane and therefore in rapid exchange with cytoplasmic rRNA. At a 28 S/18 S rRNA molar ratio in nuclei close to 1.0 this model gives the best approximation to experimentally determined specific-radioactivity curves for nucleolar and nucleoplasmic 28 and 18 S rRNA. The transfer rate (v) between the separate pools is 1.1×10^3 mol/min. The numbers in parentheses represent the amount of a given pool in molecules $\times 10^{-4}$ (above) and the respective half-life time in min (below). For details see the text.

that the rate for the small subparticle (18 S rRNA) is severalfold higher than that for the large subparticle (28 S rRNA).

The proposed model, based on the established equimolar amount of nuclear 28 and 18 S rRNA, explains satisfactorily the experimental findings showing an 18 S/28 S rRNA specific-radioactivity ratio higher than unity in the cytoplasm (Joklik & Becker, 1965; Girard *et al.*, 1965; Hadjiolov, 1966; Hogan & Korner, 1968; see Kaempfer, 1974) simultaneous with values lower than unity in the nucleus (Smith *et al.*, 1969; the present work). The fast equilibration of nucleoplasmic and cytoplasmic 18 S rRNA results in a faster transport of newly synthesized small ribosomal subparticles into the cytoplasm. On the other hand, it causes a marked dilution of the label in the nucleoplasmic pool. Further studies are necessary to assess quantitatively the correlation between the formation in the nucleus and nucleocytoplasmic transport of ribosomes with their fate in the cytoplasm.

We are indebted to Mrs. D. Kulekova and Miss A. S. Stoykova for their expert assistance in the experiments.

References

Atkins, G. L. (1972) *Biochem. J.* **127**, 437–438

Bach, M. & Johnson, H. G. (1967) *Biochemistry* **6**, 1919–1933

Brandhorst, B. P. & McConkey, E. H. (1974) *J. Mol. Biol.* **85**, 451–463

Busch, H. & Smetana, K. (1970) *The Nucleolus*, p. 626, Academic Press, New York

Chaudhuri, S. & Lieberman, I. (1968) *J. Mol. Biol.* **33**, 323–326

Dabeva, M. D. & Tsanev, R. G. (1968) *Bull. Biochem. Res. Lab.* **3**, 57–68

Dabeva, M. D., Todorov, B. N. & Hadjiolov, A. A. (1976*a*) *Biokhimiya* **41**, 458–468

Dabeva, M. D., Dudov, K. P., Hadjiolov, A. A., Emanuilov, I. & Todorov, B. N. (1976*b*) *Biochem. J.* **160**, 495–503

Dabeva, M. D., Petrov, P. T., Stoykova, A. S. & Hadjiolov, A. A. (1977) *Exp. Cell Res.* **108**, 467–471

Dabeva, M. D., Dudov, K. P., Hadjiolov, A. A. & Stoykova, A. S. (1978) *Biochem. J.* **171**, 367–374

Dudov, K. P., Dabeva, M. D. & Hadjiolov, A. A. (1976) *Anal. Biochem.* **76**, 250–258

Eliceiri, G. L. (1976) *Biochim. Biophys. Acta* **447**, 391–394

Emerson, C. P. (1971) *Nature (London) New Biol.* **232**, 101–106

Girard, M., Latham, H., Penman, S. & Darnell, J. E. (1965) *J. Mol. Biol.* **11**, 187–201

Goidl, J. A., Canaani, D., Boublik, M., Weissbach, H. & Dickerman, H. (1975) *J. Biol. Chem.* **259**, 9198–9205

Hadjiolov, A. A. (1966) *Biochim. Biophys. Acta* **119**, 547–556

Hadjiolov, A. A. (1977) *Trends Biochem. Sci.* **2**, 84–86

Hadjiolov, A. A. & Milchev, G. I. (1974) *Biochem. J.* **142**, 263–272

Hadjiolov, A. A. & Nikolaev, N. (1976) *Prog. Biophys. Mol. Biol.* **31**, 95–144

Hadjiolov, A. A., Venkov, P. V., Dolapchiev, L. B. & Genchev, D. D. (1967) *Biochim. Biophys. Acta* **169**, 129–139

Hogan, B. & Korner, A. (1968) *Biochim. Biophys. Acta* **169**, 129–139

Hunt, J. (1976) *Biochem. J.* **160**, 727–744

Joklik, W. K. & Becker, J. (1965) *J. Mol. Biol.* **13**, 496–510

Kaempfer, R. (1974) in *Ribosomes* (Nomura, M., Tissieres, A. & Lengyel, P., eds.), pp. 679–704, Cold Spring Harbor Laboratory, Cold Spring Harbor

Muramatsu, M., Hodnett, J. L., Steele, W. J. & Busch, H. (1966) *Biochim. Biophys. Acta* **123**, 116–125

Myhill, J. (1967) *Biophys. J.* **7**, 903–911

Penman, S. (1966) *J. Mol. Biol.* **17**, 117–130

Penman, S., Smith, J. & Holtzman, E. (1966) *Science* **154**, 786–789

Perry, R. P. (1976) *Annu. Rev. Biochem.* **45**, 605–630

Purtell, M. J. & Anthony, D. D. (1975) *Proc. Natl. Acad. Sci. U.S.A.* **72**, 3315–3319

Reiner, J. M. (1953) *Arch. Biochem. Biophys.* **46**, 53–99

Reiner, J. M. (1974) *Exp. Mol. Pathol.* **20**, 78–108

Sheppard, C. W. (1962) *Basic Principles of the Tracer Method*, pp. 30–47, J. Wiley and Sons, New York

Sheppard, C. W. & Householder, A. S. (1951) *J. Appl. Phys.* **22**, 510–520

Smith, S. J., Adams, H. R., Smetana, K. & Busch, H. (1969) *Exp. Cell Res.* **55**, 185–197

Toniolo, D. & Basilico, C. (1976) *Biochim. Biophys. Acta* **425**, 409–418

Tsurugi, K., Morita, T. & Ogata, K. (1974) *Eur. J. Biochem.* **45**, 119–126

Vaughan, M. H., Warner, J. K. & Darnell, J. E. (1967) *J. Mol. Biol.* **25**, 235–251

Weinberg, R. A. & Penman, S. (1968) *J. Mol. Biol.* **38**, 289–304

Weinberg, R. A. & Penman, S. (1970) *J. Mol. Biol.* **47**, 169–178

Weinberg, R. A., Loening, U. E., Willems, M. & Penman, S. (1967) *Proc. Natl. Acad. Sci. U.S.A.* **58**, 1088–1095

Winicov, I. (1976) *J. Mol. Biol.* **100**, 141–155

Wolf, S. F. & Schlessinger, D. (1977) *Biochemistry* **16**, 2783–2791

Zilversmith, D. B. (1960) *Am. J. Med.* **29**, 832–848